EMAS Engineering Modelling, Analysis & Simulation THE NAFEMS JOURNAL
NAFEMS
Vol. 3, Issue 1, 2026

Systems Simulation for Fusion Using Novel Augmented Component Mode Synthesis Reduction Techniques

Thomas Deighan[a,1], Isaac Wells[a]

[a]UKAEA (United Kingdom Atomic Energy Authority), Culham Campus, Abingdon, OX14 3DB, UK

Abstract

Systems simulation provides a valuable capability for development of any engineering asset, for targeted-fidelity rapid assessment of design concepts, upfront x-in-the-loop virtual operations and extended use into physical operations as part of a live digital twin for predictive maintenance and lifetime monitoring. This is particularly true for development of commercial fusion power plants, where limited ability for physical testing and a challenging environment for diagnostics dictates a heavier reliance on such techniques.

Realising this value will in turn rely on development of novel reduced order modelling (ROM) techniques to enable efficient simulation at an appropriate fidelity. Although advancing computational capability allows for larger and more complex simulations, the environmental and financial costs must be considered, with development of efficient ROM techniques enabling more effective use of resources including enabling the high throughput computations necessary for rigorous uncertainty quantification.

This paper presents developments of a novel full-field reduced order modelling technique using an augmented Component Mode Synthesis (CMS) reduction and modal coupling method, describing the reduction process and implementation in Modelica. The approach promises efficient simulation of coupled fluid-thermo-mechanical models of complex components within a systems environment, capturing aspects of non-linear behaviour. The approach is verified against other methods using a series of case studies, including demonstration for a coupled fluid-thermal simulation of a fusion power plant plasma facing component. Plans for further development and application for simulation of fusion systems and in wider industry are discussed in the context of moving towards realisation of a probabilistic real-time digital twin.

Keywords

Systems simulation, Reduced Order Modelling, Component Mode Synthesis, Fusion Power, Fluid-Thermal-Structural

1 Background and Motivation

Across all industries, design verification, validation and operational risk mitigation of engineering systems rely on a targeted combination of simulation and physical prototype testing. The well-known qualification pyramid (illustrated in Figure 1 in a fusion system context) illustrates this well for the design development lifecycle illustrating a progressive substantiation and risk reduction through sub-systems to the full system using a combination of simulation and test.

[1]Corresponding author.
E-mail address: tom.deighan@ukaea.uk (T. Deighan)
https://doi.org/10.59972/7g38c6hy

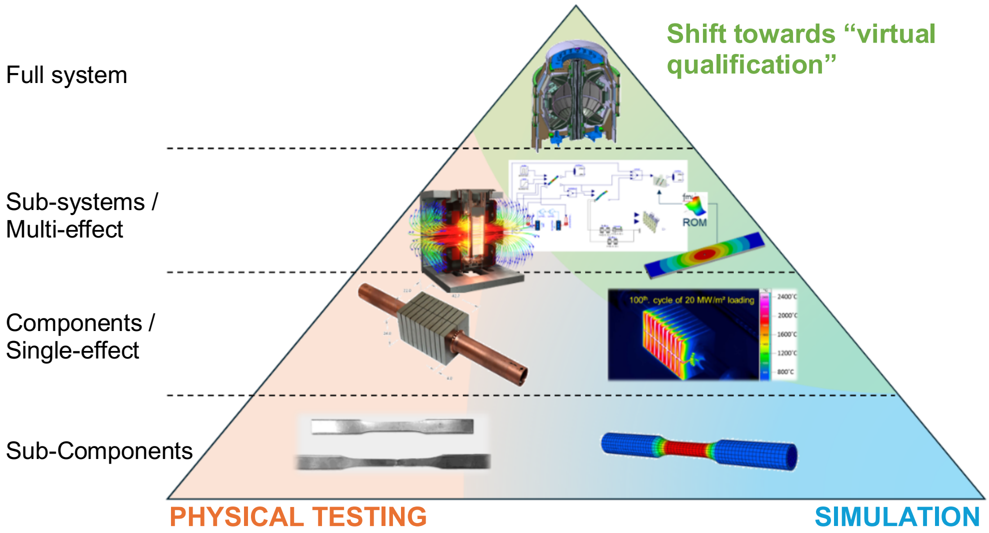

Figure 1. Qualification pyramid.

The costs and timescales associated with the physical testing increase with progression to the top of the pyramid. If deployed appropriately, any industry can stand to benefit from increasing use of simulation to shift towards "virtual qualification", especially for the larger system stages, to minimise the most expensive and time-consuming physical testing. Building confidence in these simulations may consequently rely on increasing the level of physical testing for smaller systems or single-effects, but palatable due to lower expense and shorter timescales.

Although tokamak devices have been constructed over many decades [1], they have all targeted specific experimental objectives in furthering understanding of plasma behaviour or aspects of engineering component design, but none achieve the conditions necessary for commercial power generation, requiring higher temperatures, stronger magnetic fields and longer confinement times. The tokamaks currently being designed or conceived which are planned for operation in the coming decades will be the first to demonstrate this and will be the first chance for engineering systems to be tested with full combined effects under reactor conditions.

The critical challenge for the commercialisation of fusion power is the inability to replicate, and test engineering systems in, the full environment until a fusion power reactor comes online. A significant shift towards "virtual qualification", most critically for consideration of system interactions and combined effects, is not just valuable but absolutely necessary.

Along with other simulation disciplines and techniques, systems simulation provides unique capabilities and opportunities to achieve this.

- More upfront simulation of system interactions and performance trade-offs from early concept through detailed design phases allowing for mixed and targeted fidelity and order of models
- Efficient propagation of uncertainties to enable rigorous reliability of system performance
- Ability to conduct virtual operators of full system interactions (Tokamak Simulator) and in real-time where this is needed
    - Control system design and reliability assessment
    - Concept of operational planning
    - Operator training (real-time)
    - Control room HMI design
    - Hardware in-the-loop testing (real-time)

In addition to the product design lifecycle stages, simulations can also valuably be deployed alongside in service operations to provide enhanced diagnostics for fault monitoring and predictive maintenance. In this manner the simulation is effectively deployed as a digital twin [2], providing live information alongside and learning from data from physical instrumentation.

Although the application of simulation in this regard cannot influence risk mitigation of the design of the operational device, it directly contributes to the overall risk mitigation and viability of the in-service product by improving the ability to detect potential failures and perform mitigating actions. The use of simulation in this way will be vital for the first demonstration fusion power plants by demonstrating how risks which could not be reduced further at the design stage can be mitigated during operations. This also helps address further challenges of limited accessibility or reliability of any physical instrumentation due to the harsh operating environment, consisting of extremely high temperatures, strong transient magnetic fields and neutron irradiation.

Although quasi-1d models provide valuable capability for aspects of this, especially for earlier stage concept analysis, application for more detailed design stages and certainly for in service digital-twins will rely on robust and easily deployable reduced order modelling (ROM) methods to capture more detailed behaviour. This paper focuses on developments of a new reduced order modelling technique specifically for deployment within coupled systems simulation models addressing the needs for simulation of fusion power plant systems.

2 Overview of Reduced Order Model (ROM) Methods

Reduced order modelling methods can be broadly split into two categories: model-based and data-driven.

2.1 Model-based

Model-based methods rely on a mathematical and sometimes physical understanding of the underlying problem and are derived from an analytical reduction of a high-order model. Examples include Guyan (static) reduction [3], CMS (dynamic) reduction [4], linearisation to state-space form and linear parameter-varying (LPV) models [5]. A summary is given below for reference to the developments outlined in this paper which are based on these.

2.1.1 Guyan (Static) Reduction

Considering the full order model represented by stiffness (or conductance) matrix and load vectors, it is first partitioned into retained interface DOFs, $\bar{x}_r$ and other DOFs $\bar{x}_o$,

$$\begin{bmatrix} K_{rr} & K_{ro} \\ K_{ro}^T & K_{oo} \end{bmatrix} \begin{bmatrix} \bar{x}_r \\ \bar{x}_o \end{bmatrix} = \begin{bmatrix} \bar{f}_r \\ \bar{f}_o \end{bmatrix} \tag{1}$$

Assuming the more general case of the forces on the other DOFs to be a linear superposition of a series of fixed vectors, i.e.

$$\bar{f}_o = \sum_i \gamma_i . \bar{f}_{o_i} = F_o . \bar{\gamma} \tag{2}$$

$\bar{x}_o$ can be expressed as a function of $\bar{x}_r$,

$$\bar{x}_o = G . \bar{x}_r + K_{oo}^{-1} F_o . \bar{\gamma} \tag{3}$$

and the system equations expressed as,

$$\hat{K} . \bar{x}_r = \bar{f}_r + \hat{F} . \bar{\gamma} \tag{4}$$

This is equivalent to reduce the DOF response vector as,

$$\bar{x} = \begin{bmatrix} \bar{x}_r \\ \bar{x}_o \end{bmatrix} = T . \bar{x}_r \qquad \textit{with,} \quad T = \begin{bmatrix} I \\ G \end{bmatrix} \tag{5}$$

and applying the principle of virtual work to the original equation (by multiplying through by T^T) to give the reduced stiffness matrix and reduced load vectors

$$\hat{K} = T^T . K . T \qquad \qquad \hat{F} = T^T . F_o \tag{6}$$

Providing the restrictions of the method hold true (the model is linear and stiffness matrix constant) the reduction is lossless with regards to a static analysis. A reduced mass matrix can also be calculated in the same way as $\widehat{M} = T^T . M . T$ however the correct dynamics of the system is unlikely to be captured.

2.1.2 CMS Reduction

The CMS method extends the Guyan reduction by also including a number of dynamic modes of the system. Various fundamental forms of CMS reduction exist which differ by the method used to calculate the system modes. The most commonly used is the Craig-Bampton fixed interface method outlined below. The reduction is calculated in the same way as for the Guyan reduction but with the reduction transformation given by,

$$T = \begin{bmatrix} I & 0 \\ G & \Phi \end{bmatrix}, \tag{7}$$

where Φ are the eigenvectors of the system with the retained interface DOFs $\bar{x}_r$ fixed. The reduced load vectors, stiffness matrix and mass matrix are calculated in the same way. The form of the mass and stiffness matrices are shown below.

$$\hat{M} = \begin{bmatrix} M_s & M_{sm} \\ sym & I \end{bmatrix}, \tag{8}$$

where M_s is the Guyan interface DOF reduced mass matrix and M_{sm} is the interface to modal coupling.

$$\hat{K} = \begin{bmatrix} K_s & 0 \\ sym & \Lambda \end{bmatrix}, \tag{9}$$

where K_s is the Guyan interface DOF reduced stiffness matrix, Λ is the diagonal matrix containing the eigenvalues, λ of the fixed interface normal system modes.

For a thermal analysis the stiffness and mass matrix instead relate to the conductance and capacitance of the system respectively. For a structural analysis the damping matrix can be reduced in the same way but is often calculated directly within the reduced model based on an assumption of modal or Rayleigh damping.

The eigenvalues λ have a different physical meaning depending on the physics of the model. For structural analysis problems (2nd order system), $\sqrt{\lambda}$ give the natural frequencies of the fixed boundary vibration modes, for a thermal analysis (1st order system), $1/\lambda$ refers to the decay time-constants of thermal mode shapes. Knowledge of the mode shapes and eigenvalue magnitude is used at the time of performing the reduction to make an informed decision of how many modes to include in the reduced model.

After running the reduced model within a systems simulation, the full field solution can be obtained by back-substitution using the transformation matrix T, as in Equation 5. This can be done onto the full original DOF set or onto specific DOFs or regions of interest by selecting corresponding rows from T.

2.1.3 LPV Model

A linear parameter-varying (LPV) system is a system which can be represented in state-space form with matrices which vary as a function of one or more time-varying “scheduling” parameters.

$$\begin{bmatrix} \dot{\bar{x}} \\ \bar{y} \end{bmatrix} = \begin{bmatrix} A(p) & B(p) \\ C(p) & D(p) \end{bmatrix} \cdot \begin{bmatrix} \bar{x} \\ \bar{u} \end{bmatrix} \tag{10}$$

In a quasi-LPV model the scheduling parameter $p = p(t)$ can be a function of the system states $\bar{x}$ and/or inputs $\bar{u}$. The calculation of matrices, A, B, C and D are normally specified as an interpolation over a grid of discrete linear systems (see Figure 2).

Although much of the work on LPV systems focuses on control problems (see Section 2.4), the Guyan and CMS reduced models represented by physical mass and stiffness matrices in the previous sections can all be written in state-space form and therefore potentially modelled as an LPV system.

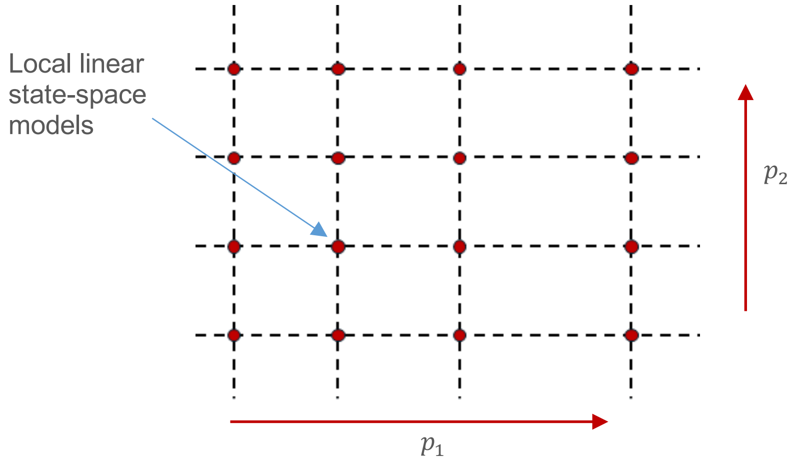

Figure 2. Grid interpolation for LPV model – for 2 scheduling parameters.

2.2 Data-driven

Data-driven models use input/output data sets from simulations of the high-order model to train the ROM, calculating the model parameters to minimise some loss function (i.e., error between the ROM and original model outputs). Some common examples are listed in Table 1.

Table 1. List of common data-driven ROM models/method.

Method	Static	Dynamic
Linear or Non-Linear regression (curve, surface or high dimensional function fitting)	Y	N
Gaussian Process Regression (GPR)	Y	N
Support Vector Machine Regression (SVM)	Y	N
Non-linear ARX	N	Y
Neural Network (MLP)	Y	N
Recurrent Neural Network (RNN / LSTM)	N*	Y
Neural ODE	N*	Y
Physical Informed Neural Network (PINN)	Y	Y

With the exception of the Neural ODEs and PINNs these models do not have any knowledge of the underlying physics or mathematical structure of the original model. Neural ODEs and PINNs, by definition, include knowledge of the underlying mathematical structure and physical problem respectively but are still data-driven models, learning parameters from the input/output data sets provided. PINN models are not considered further within this paper and remaining discussion relates more generally to the other ROM types listed.

These models may output specific scalar responses or the full field of the original model (or subset of this). In both cases the ROM is essentially the same but for the field output this data is first decomposed though singular value decomposition (SVD) [6].

$$A_{n\times N} = \sum_{i=1}^{\min(n,N)} \bar{u}_i \cdot \sigma_i . \bar{v}_i^{\,T}, \qquad (11)$$

where $A_{n\times N}$ is the data set across n spatial points and N DOE and/or time samples, $\bar{\varphi}_i$ is column i from orthogonal set of spatial mode shapes, σ_i are singular values for each mode, $\bar{v}_i$ is column i from orthogonal set of DOE/time variation vectors.

The first approximation is made by retaining the first r modes of the highest singular values.

$$A_{n\times N} \approx \sum_{i=1}^{\mathrm{r}} \bar{\varphi}_i . \sigma_i . \bar{v}_i{}^{T} = \mathrm{U}\cdot\Sigma\cdot V^{T} \tag{12}$$

The ROM is then trained using the SVD mode coefficients as the response variables in conjunction with any other scalar output responses. The process can be described with the pseudo-equation below,

$$\begin{gathered} f(\bar{\delta}_i, t_i) \xrightarrow[i=1:N]{DOE} \boldsymbol{F}_{n\times N} \xrightarrow{Truncated\ SVD} \begin{cases} \square \longrightarrow \mathrm{U}_{[n\times r]} \\ \left.\begin{array}{c} \mathrm{V}_{[N\times r]} \\ \Delta \end{array}\right\} \xrightarrow{ROM} \bar{\chi}(\bar{\delta}, t) \end{cases} \\ f(\bar{\lambda}, t) \xRightarrow{Generates} \mathrm{U}, \bar{\chi}(\bar{\delta}, t) \end{gathered} \tag{13}$$

where $\Delta = [N \times N_p]$ matrix of N_p parameter values for each DOE point $i = 1..N$, $\bar{\chi}(\bar{\delta}, t)$ = ROM function calculating SVD mode coefficients, $\bar{\delta}$ is the model parameter vector.

When the ROM is used to calculate these coefficients, they can be expanded back to the full field using the SVD mode shape matrix. The overall approximating ROM for field data can be described by the following equation,

$$f(\bar{\delta}, t) \approx f_{ROM}(\bar{\lambda}, t) = \sum_{i=1}^{r} \bar{u}_i . \bar{\chi}_i(\bar{\delta}, t) \tag{14}$$

Within the process of generating the specific ROM, the selection of design of experiment (DOE) points, number of reduced SVD modes and the particular model (i.e. from Table 1) is considered with regards to a measure of the overall model error, measured according to some verification scheme using independent verification points.

2.3 Advantages and Limitations

The various ROM methods summarised above each have specific advantages and limitations determining their applicability for different problems, which are summarised in Table 2. The main advantages of the data-driven methods are being agnostic to the physics or mathematics of the problem, allowing a wide range of applicability including use with both simulation and experimental data. The generality of these methods however provides greater challenges when looking to couple multiple models together across numerous interfaces within a larger systems model and to ensure the validity is retained and physical laws are conserved. Data-driven ROM methods are a subject of significant active research however with new and adapted techniques constantly being developed, such as in [7] and [8] for example, which has looked to address the issue of violation of conservation laws within PINNs.

Model-based methods, specifically the CMS and Guyan reduction techniques, provide a relatively simple process for exporting and deploying the ROMs within a systems environment and coupling them together. Providing the use is within the known limitations of applicability the accuracy trade-offs are well informed at build time and conservation laws are maintained. Tools for both generating and exporting these ROMs and for importing the models within an acausal systems modelling environment (i.e. Modelica or Simscape) are readily available. Despite the restrictions on applicability listed in row one of Table 2 the CMS method is widely used for structural dynamics analysis with significant published literature on the subject (see Section 2.4). In these cases, the assumptions do not restrict the method from enabling valuable insights for the specific problems and to guide design driving decisions. Although the CMS method can be applied to any problem which can be represented in state-space form it is less widely used for other physics, such as thermal analysis, most likely due to the restrictions listed in row 4 of Table 2 regarding interfacing within a systems model.

Table 2: ROM method relative advantages

Capability	Data-driven	Model-based
Applicability	+ Agnostic to the mathematics and physics of the model + Can be applied to any problem or any data, both simulation and experimental or a combination	- Applicable only to reduction from high order models which can be represented in a time-invariant state-space form - Linear material behaviour = no plastic deformation – **structural** = no temperature dependence – **thermal** - Fixed material properties (e.g. elasticity, conductivity, etc.) - Small deformations – **structural** - Fixed spatial distribution in loads and boundary conditions of non-interface DOFs - these can only vary by a scalar factor - Linear superposition of loads and boundary conditions (i.e. no synergistic effects of applied loads)
Accuracy / Robustness	- Dependant on the training set which needs to be determined by careful verification procedures - Error will normally grow significantly when moving outside of the training set (extrapolation)	+ Guyan (static) reductions are lossless providing use is within applicability + Assumptions regarding dynamic content/accuracy are known at build time by selection of eigenvalues (frequencies or time-constants) of CMS (dynamic) reduction
Build / Training	- Selection of training sets for transient models is relatively subjective and requires prior knowledge of the form of the transient loads under use - Implications of the choice of training set not easily interpretable until the time of use	+ Analytical calculation of reduced model doesn't require large training sets of data
Coupling in a systems model	- Even for small systems will require large number of ROM independent variables - even for simple static beam model will have 6 inputs and 6 outputs plus field data	+ Simple selection of interface DOFs making connection of multiple ROMs within a systems model relatively simple - Method becomes less efficient for interfaces with larger number of DOFs (i.e. connection over faces) - Coupling of thermal models to fluid models for convective heat transfer requires either the full convection interface to be included in the reduced model or for the heat transfer coefficient to be fixed and embedded in the reduced matrix.
Conservation of physical laws	- Not guaranteed to be conserved [7], [8]: force balance across mechanical model or energy balance over thermal model	+ Guaranteed to be conserved

The motivation for the work on the Augmented CMS Reduction is to explore the potential to utilise the underlying technique of the CMS reduction, exploiting the benefits this method brings, and incorporate modifications to extend its applicability to a wider set of problems. Specifically, the current work aims to extend the use to include the following cases, which otherwise are limiting for application to problems within systems models in a fusion context:

- Variable (field dependant) material properties – i.e., temperature dependant elasticity for structural analysis or neutron fluence dependant conductivity for thermal analysis
- Non-linear thermal steady-state and transient analysis (i.e., temperature dependant conductivity for thermal analysis)
- Efficient method for dealing with convective boundary interfaces for coupling with quasi-1D fluid models

2.4 Related work

From a general literature search, effort into development of ROM techniques appears to be heavily weighted towards data-driven methods and specifically neural network based methods. Before discussing the details of the Augmented CMS Reduction however, this section provides a brief overview of some related work, also aiming to extend the applicability of the CMS method.

The Augmented CMS reduction method for structural analysis was first introduced by the author in [9], presented at the NAFEMS Multi-Physics Conference 2023. In this, the use and limitations of a Guyan reduction for systems level static structural analysis is discussed and the Augmented CMS Reduction technique introduced to extend the use to cases where the material properties vary as a function of temperature. A general approach to build single physics ROMs and couple them through the ROM modes into a multi-physics system model is also shown and more specifically a process for coupling the static Guyan reduction to an upstream thermal ROM and downstream data-driven reduced order sub-model for localised plastic stress calculation. The work demonstrated excellent accuracy (<0.1% error) on an initial verification case, with significant run-time advantage over the full order model (26,000 reduced CPU time). The outline of further work included extension of the technique to thermal analysis, which is the main focus for this paper.

Much of the work developing and deploying LPV models is focused on development of control algorithms. The relative merits of data-driven and model-based approaches to ROMs of lithium-ion batteries is discussed in detail in [10] and a LPV based method is developed to maintain the benefits of the model-based ROM approach whilst enabling aspects of non-linear behaviour to be captured.

There has been some work to develop upon the standard CMS method by application of LPV model concepts. In [11] the CMS method combined with LPV techniques are used to perform transient analysis of structures with plastic deformation at reduced computational cost. In [12] the CMS method is combined with LPV techniques to capture the effect of design parameters on structure dynamics response by direct interpolation of CMS matrices.

In [13] and [14] CMS methods are deployed for thermal analysis of turbine blades but with convection loads embedded within the FEA model. The majority of published work utilising CMS methods is regarding structural analysis however.

The Augmented CMS Reduction method as introduced in [9] is essentially a form of LPV model applied to the Guyan reduction matrices and generalising the "interpolation" of system matrices to use any data-driven ROM technique and utilising SVD of the matrix data to reduce the dimensionality. This paper defines variations of the Augmented CMS method, extending to the more general CMS reduction case, applying them to thermal problems and developing associated interface reduction techniques for convection boundaries.

3 Augmented CMS Reduction Method

A standard CMS reduction results in the set of matrices shown in Table 3 which form the reduced model.

Table 3. CMS model matrices.

K_s	$n \times n$	Guyan (static) interface DOF reduced stiffness matrix
M_s	$n \times n$	Guyan (static) interface DOF mass matrix
M_{sm}	$n \times m$	Interface to modal coupling mass matrix
$\bar{\lambda}$	m	vector eigenvalues of the fixed interface normal modes
$\hat{F}$	$(n+m) \times l$	set of reduced load vectors for each scalable loadcase $[1..l]$
G	$n_0 \times n$	Constraint mode and fixed boundary normal mode shapes forming the transformation (back-substitution) matrix
Φ	$n_0 \times m$	

$n =$ number of reduced interface DOFs
$m =$ number of modes
$l =$ number of reduced load vectors
$n_0 =$ number of DOFs in original model

The augmented reduction method deals with cases where these matrices vary according to parameters which will be time-varying (potentially form upstream connected ROMs) within the deployed systems model.

A DOE is run on the original high order model with CMS reduction data generated for each DOE point. The DOE does not need to form a regular grid, with sample points selected based on the type of augmented reduction and the data-driven ROM method used in the following step.

Where the variation of this data is sufficiently small over the DOE space the matrix can be assumed constant and set to some average or nominal value from the DOE samples. Where the variation will lead to significant change in the static or dynamics response the data from each matrix is modelled using an appropriate data-driven ROM method (such as from Table 1). An SVD is performed on the matrix data to reduce the dimensionality of the ROM ($r < k$) and exploit the underlying relationships governing the variation in the stiffness and mass data.

$$\xrightarrow[i=1:N]{DOE} \left\{ \begin{array}{l} \boldsymbol{D}_{k\times N} \xrightarrow{Truncated\ SVD} \left\{ \begin{array}{l} \square \longrightarrow \boldsymbol{\Psi}_{k\times r} \\ \mathbf{V}_{N\times r} \end{array} \right. \\ \longrightarrow \boldsymbol{\Delta}_{N\times N_p} \end{array} \right. \left. \right\} \xrightarrow{ROM} \bar{\chi}_r(\bar{\delta}) \quad (15)$$

$\boldsymbol{D}_{k\times N} =$ data from each of the CMS model matrices shown in Table 3, reshaped into vectors for each DOE point $[1..N]$.

The data within the matrices varies only due to the variation in the terms of the stiffness and mass matrix of the original model which in most applications will be governed by the material property models. In these cases the form of these variations therefore relates directly to the form of the material property functions. The exception to this is when the parameters relate to geometric parameters of the model.

To ensure the force or energy balance over the reduced model is conserved, for the static stiffness matrix, data is taken as

$$\boldsymbol{D} = K_{sU} \qquad \text{where,} \qquad K_s = K_{sU}^T + K_{sD} + K_{sU} \quad (16)$$

and K_{sU} is strictly upper triangular, and K_{sD} is diagonal. The removal of the n values within K_{sD} from the SVD is replaced by adding n constraints within the implemented Augmented CMS model, constraining the sum of the matrix columns/rows to zero.

For the static mass matrix $\boldsymbol{D} = M_{sU}$ to exploit the symmetry. For all other matrices the full data is used for the SVD.

As the eigenvalues for each normal model $\bar{\lambda}$ change differently across the DOE the order of the modes within Φ may change and therefore also the column ordering of data within M_{sm}. Therefore, prior to building the ROMs for this data a Modal Assurance Criteria (MAC) analysis is performed to determine the equivalence of the modes across the DOE space and then the data reordered and sign flipped accordingly to ensure equivalence.

3.1 Parameter Varying Augmented CMS

For a Parameter Varying CMS (PV-CMS) the parameters are independent of the sates of the CMS model. In this case the build of the model is conducted according to the process outlined previously with a series of CMS reductions performed across the parameter space as dictated to build a data-driven ROM of acceptable accuracy and according to the ROM verification strategy. Use cases include examples outlined in Table 4 below.

Table 4. Example use cases for PV-CMS model.

Model Physics	Parameters	Load vectors
Thermal	Irradiation dpa field mode coefficients – effecting material properties	Volumetric neutron heating mode shapes
Structural	Temperature field mode coefficients – effecting material properties Irradiation dpa field mode coefficients – effecting material properties	Temperature field mode shapes
Any	Geometric parameters (Requires mesh morphing and interpolation for consistent back-substitution model)	

Implementation within a thermal systems model component is shown in Figure 3 below.

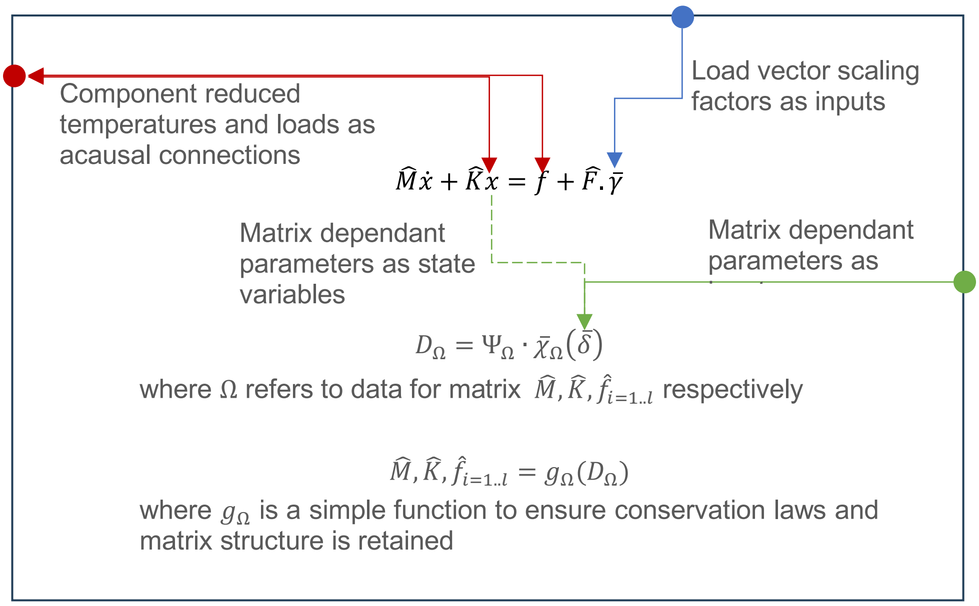

Figure 3. Augmented PV-CMS implementation for thermal analysis.

3.2 State Varying Augmented CMS

For a State Varying CMS (SV-CMS) the parameters consist of or include the CMS model states. This extends the use to non-linear cases (i.e. where material properties are state dependant). The DOE set of the full order model needs to ensure the state response space is suitable covered. This is achieved by a series of steady state simulations to cover the space of the interface DOF states and a number of transients simulations with step inputs on the interface DOFs in order to trigger response of the modal DOFs. CMS reductions are performed on perturbed full system matrices under the steady state solution and at various time points within the transients.

The reduced interface and modal DOF state responses are calculated from the full order model responses at each DOE point i, by projection,

$$\begin{bmatrix} \bar{x}_r \\ q \end{bmatrix}_i = (T_i{}^T . T_i)^{-1} \cdot T_i{}^T \cdot \bar{x}_i \tag{17}$$

Handling of scaled load vectors necessitate a modification to $\bar{x}_i$ within the above equation but is omitted form the above for simplicity and not implemented as part of the work presented here.

The primary use case explored within this work, is thermal analysis with temperature dependant properties. Implementation within the systems model is the same as for the PV-CMS but with the model states internally connected (equated) to the parameter inputs (see dotted green line in Figure 3).

3.3 Convection Boundary Interface Reduction

As part of preparing CMS models, assumptions are normally made regarding creation of the interface DOFs to be retained, to minimise the number of retained DOFs in the reduce model.

RBE3 (average/flexible) and RBE2 (rigid) style constraints are often used to condense a node set of the original model down to a single node to be retained. For a thermal model this is equivalent to enforcing a uniform heat flux and enforcing a uniform temperature across the set respectively. Higher order constraints can be employed however to retain more freedoms in the reduced model, such as utilising two parent nodes to allow a linear gradient of heat flux or multiple nodes allowing a heat flux pattern according to a defined shape function controlled by the parent nodes. A particular issue however, as highlighted in Table 2 is dealing with convection boundaries of thermal models. If the convection load is included within the original model the stiffness matrix becomes dependent on the heat transfer coefficient (HTC). This could be handled using a PV-CMS with the HTC acting as a parameter however this has several shortcomings:

- does not easily permit HTC models with wall temperature dependency
- does not easily permit HTC models with spatial variations as a function of flow configuration
- likely to lead to more complex data-driven ROMs for the stiffness matrix and harder to enforce conservation laws, especially if temperature or spatial dependency is included

The method outlined here attempts to provide a scheme to enable efficient handling of convection boundary interfaces such that the HTC does not become a direct parameter of the PV-CMS and is not embedded and fixed within the reduced model.

A first set of CMS reductions are created across the DOE space, as detailed in previous sections, with the full convection boundary included. If the model is otherwise a standard CMS (i.e. not parameter or state varying) then instead a single initial CMS reduction is generated and a DOE run using the reduced model, reducing the computational resource required. The DOE must cover suitable variations in HTC as governed by the HTC model, however the HTC itself or parameters of the HTC model are not used directly in the interface boundary reduction.

An SVD is performed on the DOF heat flux loads of the full convection boundary set.

$$X_{cf\,[N_f \times N]} = U_{cf} \Sigma_{cf} V_{cf}{}^T \tag{18}$$

The first $r \leq \min(N_f, N)$ SVD modes are retained based on assessment of the truncation error in approximating the response of the full DOF set. A selected subset of $N_r \leq r$ DOFs from the full convection boundary set are selected and an SVD is performed on the reduced set.

$$X_{cr\,[N_r \times N]} = U_{cr} \Sigma_{cr} V_{cr}{}^T \tag{19}$$

Linear correlation coefficients are calculated between the modal response vector V of the full and reduced set,

$$\bar{c} = diag(V_{cr}{}^T \cdot V_{cf}) \tag{20}$$

Which relate the modal amplitudes of the reduced set α to the full set β,

$$\alpha_i = c_i . \beta_i \tag{21}$$

The heat loads on the full boundary can be represented in terms of modal freedoms of the set,

$$\bar{f}_{cf} \approx \sum_i (\bar{a} \odot \bar{u}_{cf\,i}) . \alpha_i \tag{22}$$

where $\bar{a}$ is a vector of effective nodal areas and $\odot$ indicates element wise multiplication as per the .* operator in Matlab.

The modal amplitudes of the reduced convection boundary set can be calculated by resolving the heat loads on those DOF's into modal coordinates (projecting the loads onto the modal freedoms),

$$\beta_i = (\bar{u}_{cr_i}^T \oslash \bar{a}_r) . \bar{f}_{cr} \tag{23}$$

where $\bar{a}_r$ is a vector of effective nodal areas of the reduced set and $\oslash$ indicates element wise division as per the ./ operator in Matlab.

Substituting Equations 23 and 21 into 22 gives,

$$\begin{aligned} \bar{f}_{cf} &\approx \sum_i (\bar{a} \odot \bar{u}_{cf_i}) . c_i . (\bar{u}_{cr_i}^T \oslash \bar{a}_r) . \bar{f}_{cr} \\ &= (U_{cf} . U_{cr}{}^T) \odot \bar{c} \odot (\bar{a} . (1 \oslash \bar{a}_r)^T) . \bar{f}_{cr} \\ &= P . \bar{f}_{cr} \end{aligned} \tag{24}$$

The matrix P projects loads acting on the reduced convection boundary DOFs to the full convection boundary, effectively constraining the loading distribution to the limited set of modes selected. A second stage Guyan reduction is then performed on the CMS models, removing unwanted convection boundary DOFs, to produce an Augmented CMS with Convection Boundaries (CMS-CB).

A new set of reduced model matrices are produced as per the list in Table 3 and a second Guyan constraint mode matrix, G_{21} is produced which calculates the removed convection boundary DOFs from the remaining interface DOFs. Assuming the first stage reduction DOFs to be arranged as $[x_r, x_{co}, q]$, the overall transformation matrix, back to the original model, is given by,

$$T = \begin{bmatrix} \begin{bmatrix} I \\ G_{12} \end{bmatrix} & 0 \\ \begin{bmatrix} G \cdot \begin{bmatrix} I \\ G_{12} \end{bmatrix} \end{bmatrix} & \Phi \end{bmatrix} \tag{25}$$

where x_r are the retained interface DOFs, x_{co} are the removed convection boundary DOFs and q is the modal DOFs.

The constraints imposed by P can be incorporated into the model for the second stage reduction in different ways.

1) P can be used directly as a load projection matrix and reduced as per any load vectors within the model. An additional matrix is added to the reduced model data set as the "reduced convection boundary load projection matrix" given by,

$$H = [I \quad G_{12}{}^T] \cdot \begin{bmatrix} P_r \\ P_o \end{bmatrix} \tag{26}$$

2) P can be used to form a constraint equation added to the system in the form,

$$P'^T . \bar{x}_{cf} = \bar{x}'_{cr} \tag{27}$$

where $\bar{x}'_{cr}$ is a new set of DOFs representing the retained convection boundary DOFs. Corresponding rows from G_{12} are then used to calculate $\bar{x}_{cr}$ from $\bar{x}'_{cr}$ needed to interface with a convection heat transfer model inside the coupled systems model.

Each method has its advantages and disadvantages in terms of implementation of the CMS-CB model and back-substitution model. Both have been implemented and show similar accuracy. Implementation of the projection method within the thermal systems model is as shown in Figure 3 but with appropriate ordering of the DOFs and the heat balance equation replaced by,

$$\hat{M}\dot{x} + \hat{K}x = \begin{bmatrix} \begin{bmatrix} I \\ 0 \end{bmatrix} & H \end{bmatrix} . f + \hat{F} . \bar{\gamma} \tag{28}$$

and the matrix H added to the list defined by Ω.

4 Verification

The PV-CMS was previously implemented in a FlexibleBody library in Modelica and verification cases presented in [9]. For this work it was implemented along with the SV-CMS and CMS-CB variants within a ThermalBody library in Modelica. Additional tools were developed in Python and Matlab to enable efficient export of the CMS data from FEA codes and processing of the data respectively. Matlab was used to process the data as required by the Augmented CMS models, including building the matrix data-driven ROMs.

To provide initial verification of the method for use with thermal simulations, two simple test cases were created to verify the SV-CMS and CMS-CB implementations separately. Accuracy and run-time of the results are compared to the original high order model and to an alternative ROM using a purely data-driven method.

4.1 Test Case 1A: Steady heat transfer along a bar

The FEA model used is shown in Figure 4. The material is Pure Copper with a linearly reducing conductivity with increasing temperature.

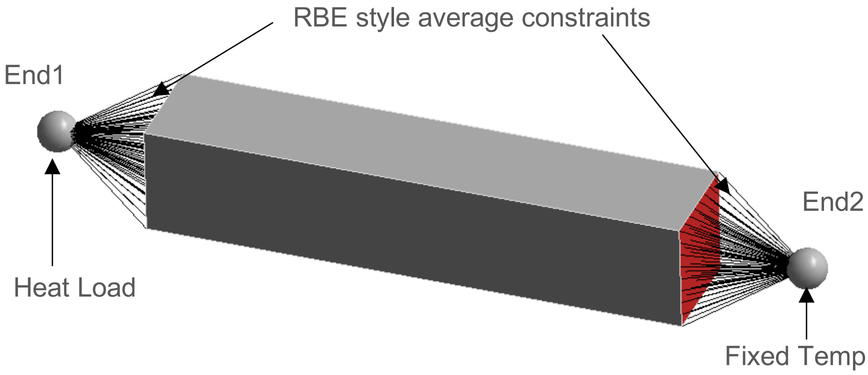

Figure 4. Test Case 1 FEA model.

The results for the End 1 temperature are shown in Figure 5 compared to the full order model results. Two SV-CMS models were built, a) using an 11-point DOE, and b) using a subset of only 3 points, marking the extremes of the DOE space. The model was run across the points used to train the model and any unused DOE points plus 9 randomly selected points for independent verification. These are shown separately by the (blue) and (orange) points respectively. For reference the model was also run using a standard CMS model with data fixed at room temperature (grey).

The results show very good performance with an RMS and Max error of 0.33% and 1.42% compared to 5.75% and 10.16% respectively if non-linear behaviour is ignored (ie. standard CMS). Heat flux at End 2 is not plotted as this has zero error due to the model maintaining energy conservation.

The CPU-time of the SV-CMS model was approximately 4000 times less than the full order FEA model.

To provide a comparison to an alternative data-driven method a standard Kriging GPR model was generated using the Surrogate Modelling Toolbox (SMT) [15]. The default options for the model were used. A set of 18 DOE points were generated consisting of 9 Central Composite Design (CCD) and 9 Optimal Space Filling (OSF). To assess the dependence on model performance with number of training points successive ROMs were constructed, trained on a subset of this DOE and verified on the remaining points. In each case this was repeated up to 150 times using a different randomly selected subset. In all cases 3 of the original CCD points were always maintained within the training set, marking the extremes of the DOE space. The errors are compared to the SV-CMS method in Figure 6. The markers show the RMS error across the verification tests and the bars show the maximum, indicating the range of error across the verification cases.

The results show that the GPR method achieves a similarly low error to the SV-CMS method with >12 training points, but this error grows, where that of the SV-CMS method holds, for reduced training set sizes. The maximum error and therefore error range across the verification cases is significantly larger for the GPR method. Above 10 training points the GPR method is able to predict the heat flux well but below this the error grows rapidly, violating energy conservation of the model.

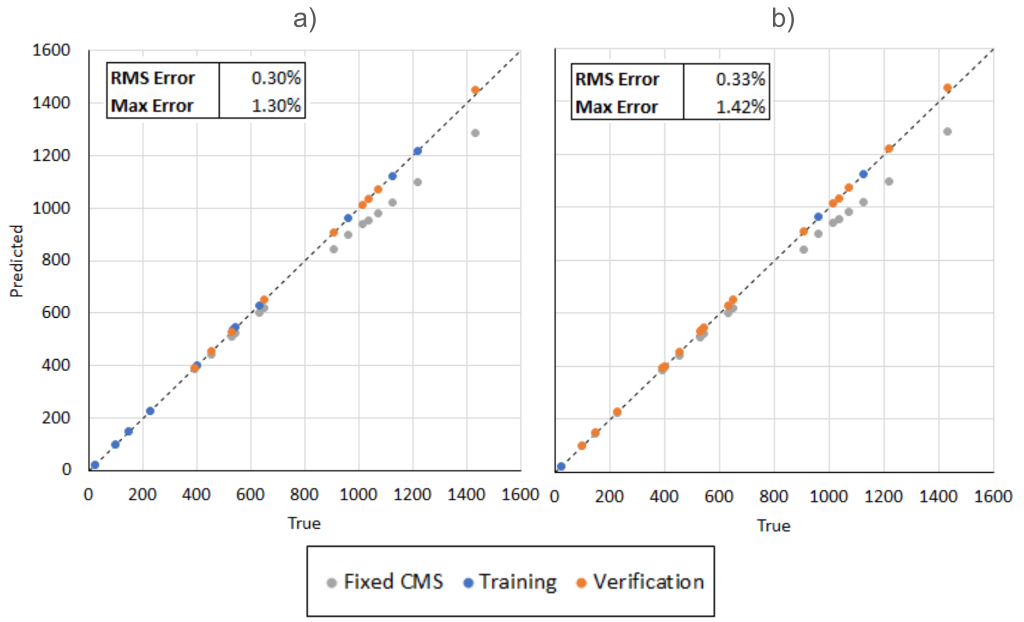

Figure 5. Test Case 1A - predicted vs actual temperature at End 1, a) using all training points, b) using subset of 3 points.

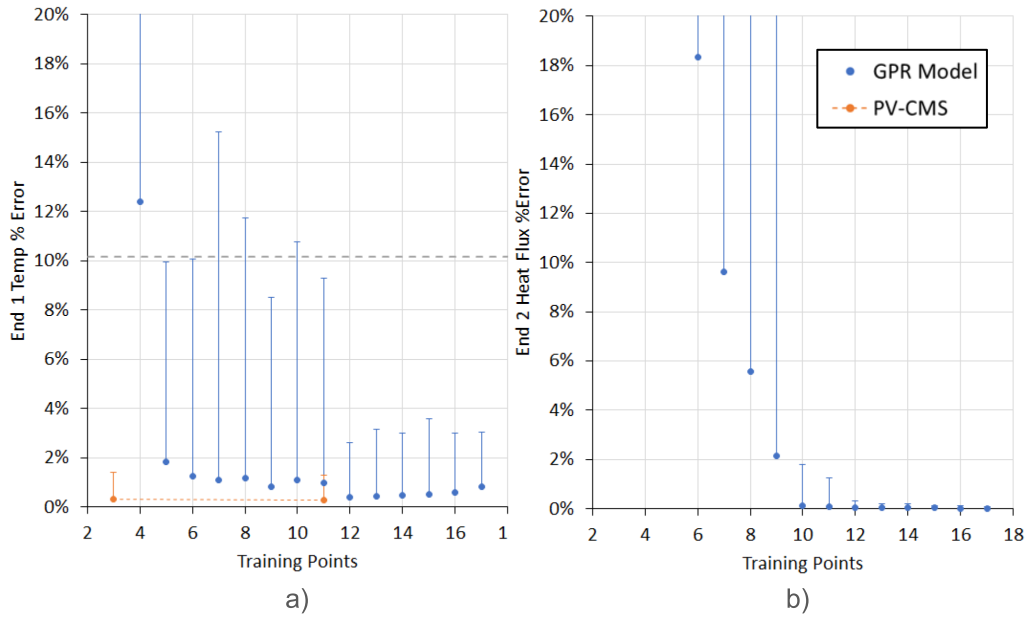

Figure 6. Test Case 1A - Comparison of results to GPR method, a) End 1 Temperature, b) End 2 Heat flux.

4.2 Test Case 1B: Transient heat transfer along a bar

The same model used for Test Case 1A was used.

For reference a comparison of the high order model results with constant (values for 22 degC) and non-linear conductivity is shown in Figure 7. The results show a growing deviation with increasing temperature as would be expected, up to a maximum error of ~11%.

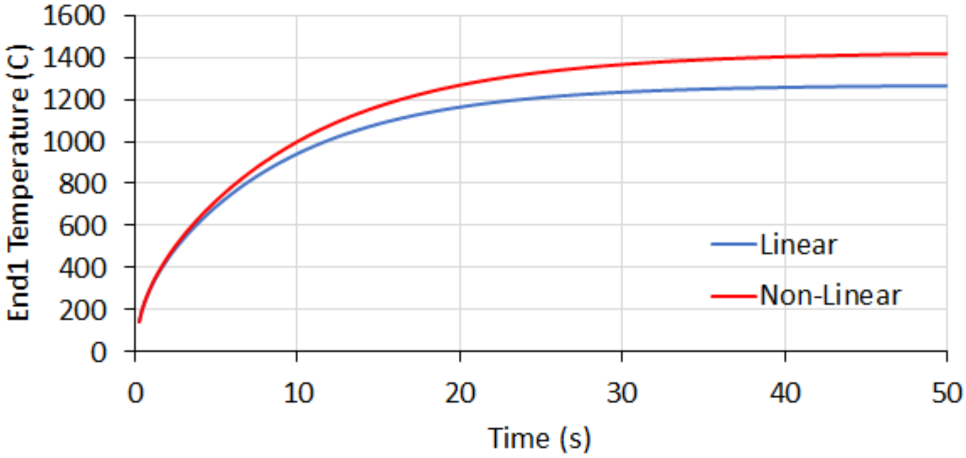

Figure 7. Test Case1B - reference high order FEA model rsults with linear (fixed at values for 22 degC) and non linear (temperature dependant) conductivity.

A standard CMS model was first run to confirm the choice of the number of dynamic modes. Figure 8 shows a comparison of the linear high order model with the CMS results with 1 mode and no modes (i.e. Guyan reduction only).

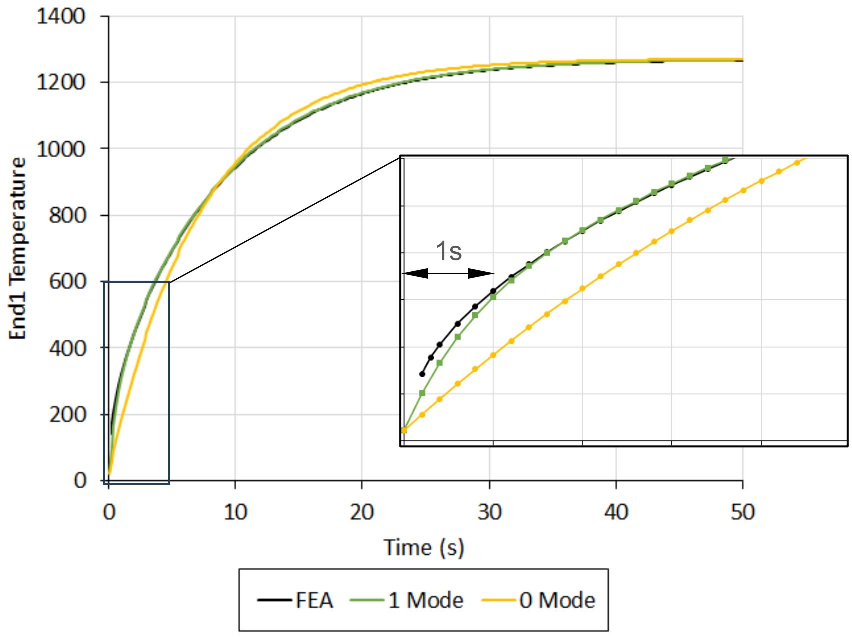

Figure 8. Test Case 1B - effect of number of modes on CMS error.

The comparison shows 1 mode is able to provide good accuracy with the only significant loss of accuracy occurring during the 1.5 sec of the transient due to response of lower time constant modes which have suitable decayed beyond that time.

An SV-CMS model was therefore constructed consisting of 1 mode. The model was trained on 6 DOE points consisting of the same 3 steady state cases used for Test Case1A with an additional 3 consisting of time samples at 1, 4 and 8 sec from a transient simulation with a step change in heat flux at End 1. Four independent verification cases were generated each consisting of two sequential step changes in heat flux followed by a ramp in heat flux. For the first test case specific values were chosen for the amplitude and time periods, with that of the other three selected at random. The results for the first verification case are shown in Figure 9 with a comparison of the relative error for all verification cases shown in Figure 10. The error for case 1 from neglecting non-linearity completely (i.e. standard CMS) is overlayed for context.

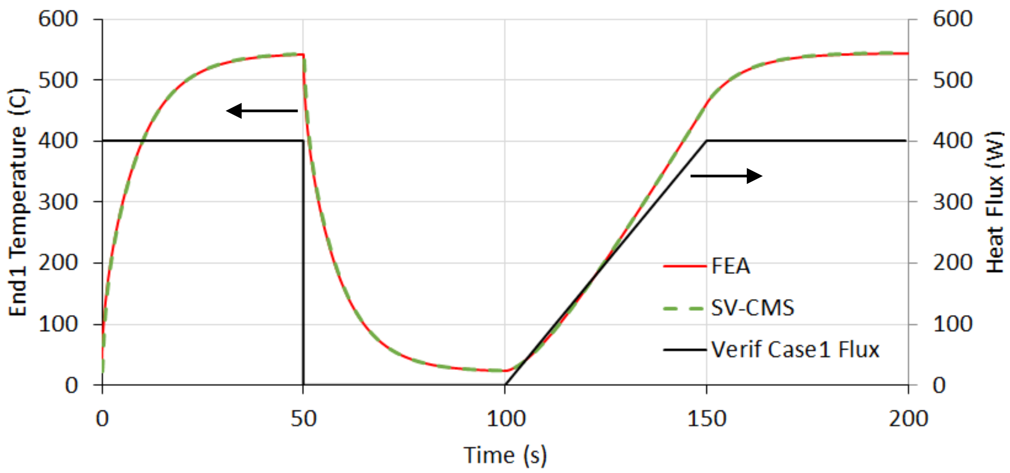

Figure 9. Test Case1B - Verification case 1 results.

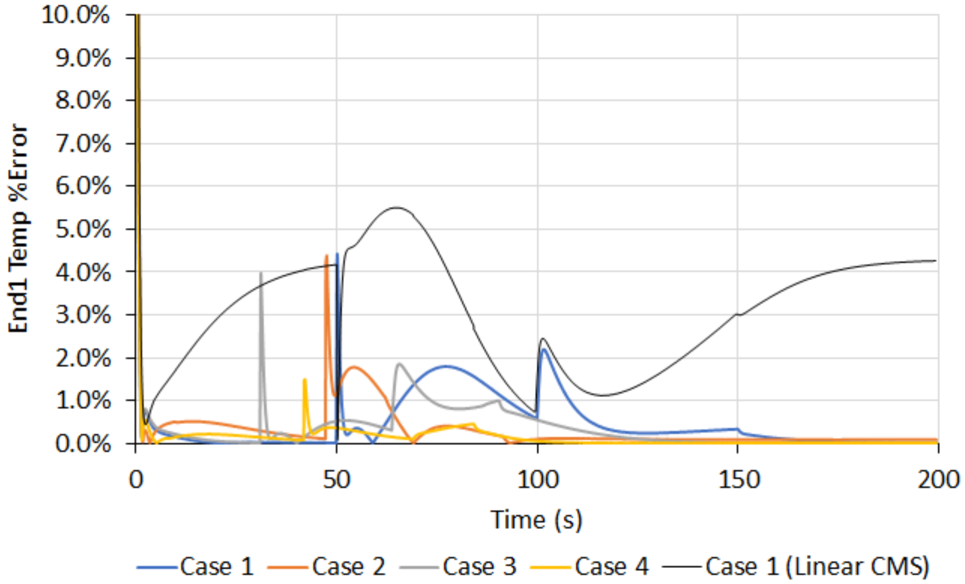

Figure 10. Test Case1B - Verification case % error.

The results show good performance over the verification cases with the maximum % error staying below around 2% except for the short (<1.5s duration) peaks due to the modal truncation of the CMS. These are seen to decay following the specific event (step / ramp) and the ROM is able to achieve good accuracy in steady state response (as per the steady state test case). In contrast, if non-linearity is neglected completely the errors are consistently above 1%, maximising at around 5% and simply grow with increasing temperature.

To provide a comparison to an alternative data-driven method a ROM was constructed using Ansys Twin Builder, employing a proprietary method related to a NARX recurrent neural network [16], [17].

Two ROM variants were constructed, one trained only with different magnitudes of step change in heat flux, and the other with a collection of training scenarios covering different variations of steps and ramps of heat flux in both directions, designed to be a more optimum training set. These were run over the same verification cases, with the results shown in Figure 11 a) and b) respectively, again with the error for case 1 from neglecting non-linearity completely, overlayed for context.

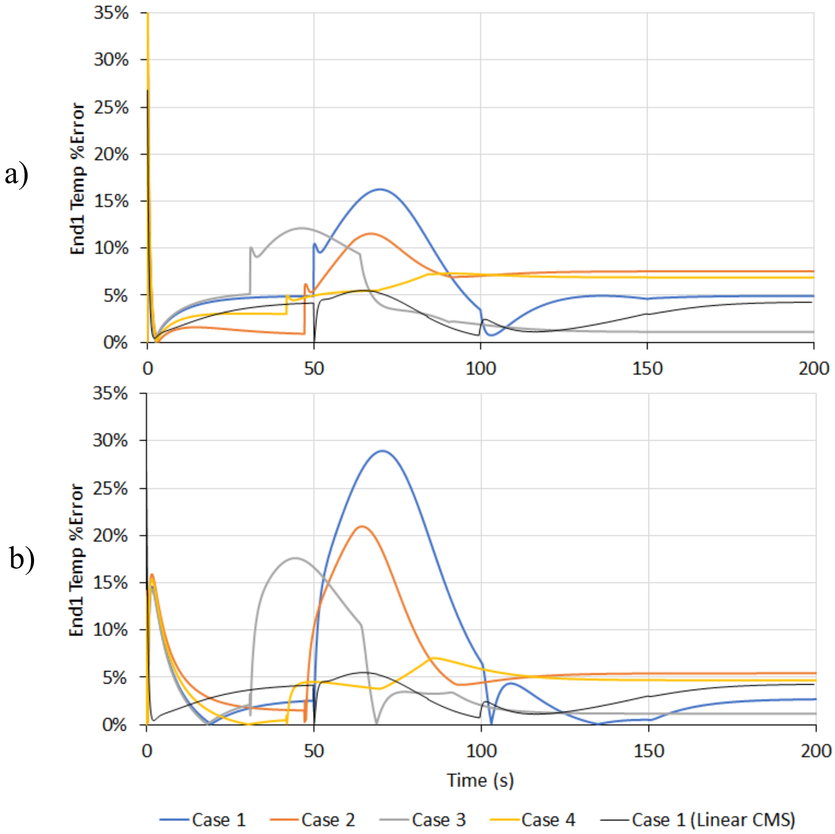

Figure 11. Test Case 1B - Comparative results from data-driven Neural Network based ROM with a) training set limited to step change increase and b) varied training set including step and ramp increase and decrease.

The results are seen to give peak errors (ignoring initial short duration spikes) of around 15% to 30% for the limited and more optimal training sets respectively. In contrast to the SV-CMS method the errors can be seen to be longer lived showing the difficulty in the ROM achieving both dynamic accuracy and correct steady state response. Looking at case 1 the errors are also seen to be larger than that if non-linearity is neglected completely. This conclusion implies that, for this case, neglecting non-linearity and using a standard CMS would be more accurate. More generally therefore the accuracy of a data driven dynamic model should be considered in context of the error form neglecting non-linearities all together under which a standard CMS will perform very well.

Figure 12 shows a summary of the time averaged and standard deviation in error for each case for the SV-CMS ROM and data-driven ROM. This shows the SV-CMS ROM performing significantly better (5-10 times reduced error) over all test cases. The more optimal training set for the data-driven ROM shows a generally higher error but this is not consistent across all cases. Although a more accurate data-driven ROM may be achievable with further optimisation of the training set it can be easy for this to lead to over-fitting and starts to require more detailed up-front knowledge of the transient loading in use. The limited training set needed for the SV-CMS method to achieve considerably better accuracy is seen as one of the main proposed advantages.

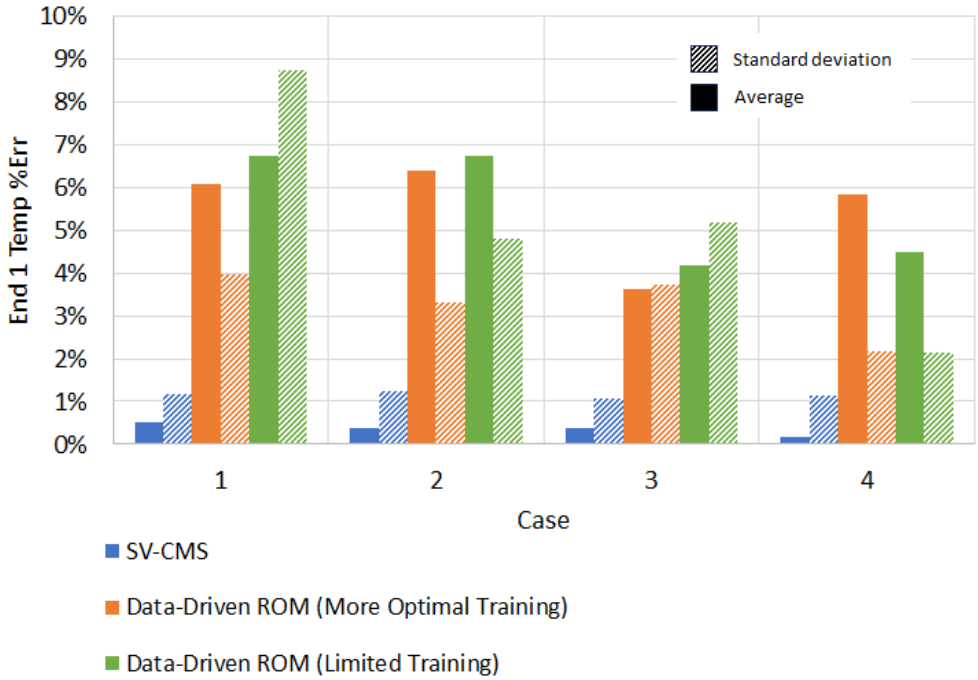

Figure 12. Test Case 1B - Comparison of SV-CMS and data-driven ROM method

The CPU-time of the SV-CMS model was approximately 4000 times less than the full order FEA model.

4.3 Test Case 2: Steady heat transfer through fusion plasma facing component with convective cooling

The steady state thermal FEA model used for this case is shown in Figure 13. The material properties were constant and fixed, with this case verifying the approach to the convection boundary reduction only.

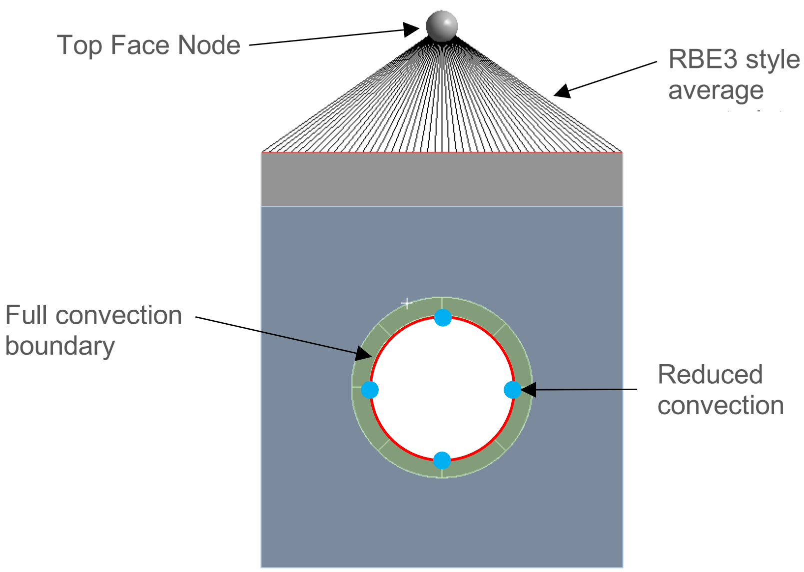

Figure 13. Test Case 2 FEA model.

As the model is linear and steady state a single CMS was exported, with the top face and full convection boundary set included as interface DOFs. No modes were included and is therefore essentially a Guyan reduction. The reduced model was run over a DOE covering a range of heat fluxes applied to the top face node and a range of heat transfer coefficients (HTCs) applied to the convection boundary nodes.

A CMS-CB ROM was constructed using the method outlined in Section 3.3 for a number of different DOE sizes to show the dependence on accuracy on the training set size. A full set of 100 points was generated. In each case a subset of DOE points was selected at random from this initial set and used to build a CMS-CB ROM, which was then run and verified on all 100 points. This was repeated 100 times for each case to gather statistics on the maximum and average error to avoid skewed results due to an unintentional favoured DOE subset selection. A model was also generated and run using all 100 points. To provide a comparison to an alternative data-driven method a GPR model was built using the same method as detailed in Test Case 1A but this time with 151 training points consisting of the same 100 points used for the CMS-CB ROM and an additional 51 point generated by OSF method.

The evaluation of error resulting from the SVD on the convection boundary heat flux is shown in Figure 14. Based on this 2 SVD modes were used, with the corresponding mode shapes shown in Figure 15.

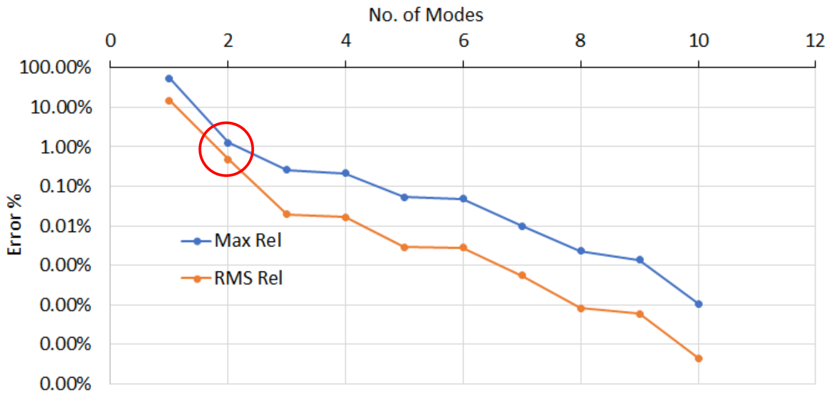

Figure 14. Test Case 2 - SVD error on convection boundary.

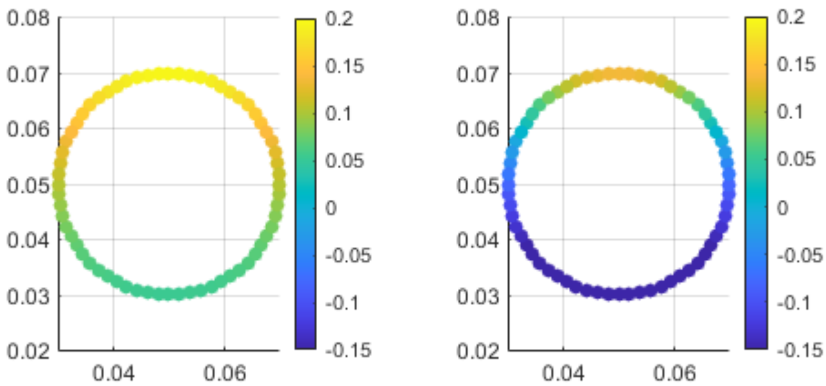

Figure 15. Test Case 2 - Convection boundary SVD mode shapes.

A comparison of the relative error in the top face average temperature is shown in Figure 16. The data for the CMS-CB model shows the maximum error occurring across the verification cases with the marker and bars giving the maximum and standard deviation across all 100 repeats respectively. The data for the GPR model shows the average error (marker) and standard deviation (bars) across all verification cases and repeats for each training set size.

The GPR model is shown to need around 70 training points to achieve an error of below 5%, with an approximately exponential trend in error as the training size is reduced. The CMS-CB method shows error below 1% down to less than 10 training points. This demonstrates one of the potential advantages of the boundary reduction method in being relatively undemanding with regards to the training data as the model itself is not being trained on the data and instead the data just needs to be sufficient to achieve a correlation of the full and reduced convection boundary set.

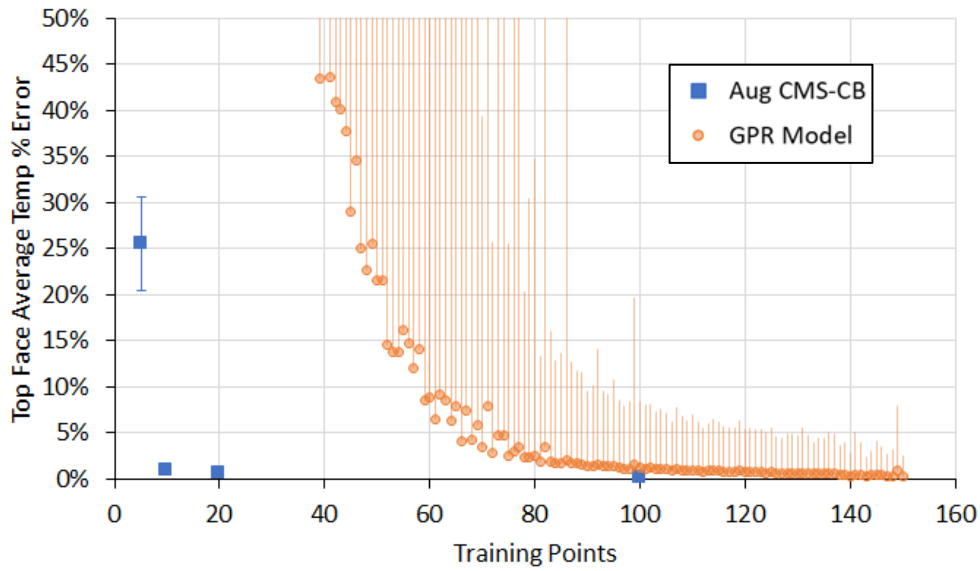

Figure 16. Test Case 2 - Comparison of top face temperature % error with alternative data-driven GPR model.

5 Conclusions & Further Work

This paper has provided an overview of the critical role that system simulation will play for fusion power plants during both design and operational phases. The Parameter Varying Augmented CMS (PV-CMS) was introduced initially in [9], implemented in Modelica, for application to structural analysis. This method was further extended here for application to non-linear steady and transient thermal analysis using a State Varying Augmented CMS (SV-CMS), implemented in Modelica. A method was also presented to enable efficient reduction of convection boundary interfaces (CMS-CB).

Application of these methods to an initial set of verification cases showed better accuracy and reduced training demand when compared to some alternative data-driven approaches. There are many existing data-driven methods which are constantly being advanced and new methods being developed. Therefore, although it is likely possible, with further optimisation of the training, detailed settings etc., that a similar accuracy could be obtained with data-driven methods, the Augmented CMS approach has potential to maintain the advantages of the standard CMS method whilst removing some of the critical drawbacks regarding non-linear behaviour and interface reduction. Although the method introduces some level of data-driven training this should be much less demanding and less subjective, especially for transient models and dealing with convection boundaries. This was borne out from the initial verification cases which showed substantially reduced requirement on the number of training simulations and reduced variation/sensitivity to the particular training points used. Further work would be needed to provide a more quantitative measure of the relative training effort and establish how this comparison changes as the models become more complex and the size of the parameter space increases.

A direct comparison of ROM simulation CPU-time was not made between the Augmented CMS methods and purely data-driven approaches, for which to do so fairly would require both to be implemented within the same systems simulation environment. However, to quantify the general purpose of pursuing the development and use of ROM methods for system simulation, as with the results reported in [9], a comparison of CPU-time with the full-order method showed substantial speed up, which would be expected to grow significantly with larger models.

Further work is needed to conduct more extensive and progressively more complex verification tests, including benchmarking to other available methods. In parallel the method will be deployed on active work developing systems models of fusion power plant systems such as that shown in Figure 17 of a coupled thermal-structural-fluids model using the plasma facing component from Test Case 2. Models such as this will be used both for design and in conjunction with other developments, towards use of systems simulation for a power plant digital-twin.

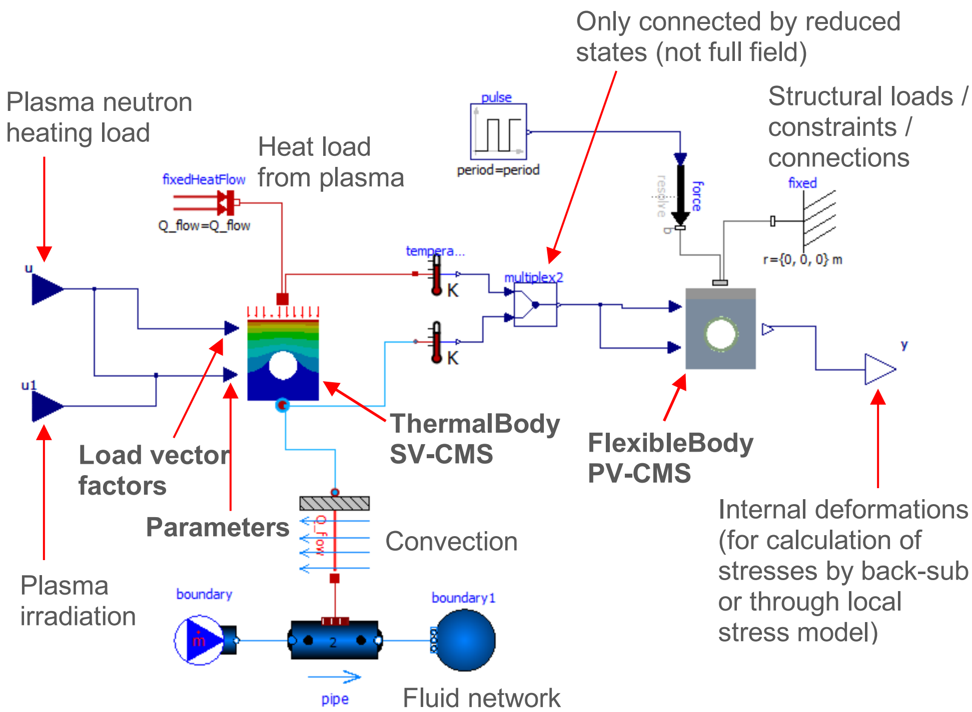

Figure 17. Example application for systems model of plasma facing component.

6 Nomenclature

ARX	Autoregressive Exogenous Neural Network
CMS	Component Mode Synthesis
CMS-CB	Augmented CMS with Convection Boundaries
DOE	Design of Experiments
DOF	Degree of Freedom
FEA	Finite Element Analysis
GPR	gaussian Process Regression
HTC	Heat Transfer Coefficient
LPV	Linear Parameter Varying
LSTM	Long Short-Term Memory
MAC	Modal Assurance Criteria
MLP	Multilayer Perceptron
NARX	Nonlinear Autoregressive Exogenous Neural Network
ODE	Ordinary Differential Equation
PINN	Physics Informed Neural Network
PV-CMS	Parameter Varying CMS
RNN	Recurrent Neural Network
ROM	Reduced Order Model
SMT	Surrogate Modelling Toolbox
SV-CMS	State Varying CMS
SVD	Singular Value Decomposition
SVM	Support Vector Machine

7 References

[1] IAEA, “World Survey of Fusion Devices 2022,” 2022. [Online]. Available: https://www-pub.iaea.org/MTCD/Publications/PDF/CRCP-FUS-001webRev.pdf.

[2] T. Deighan, “What is a Digital Twin,” [Online]. Available: https://doi.org/10.14468/g37s-ds92.

[3] R. Gujan, “Reduction of stiffness and mass matrices,” *AIAA Journal,* vol. 3, 1965.

[4] R. Craig and C. Bampton, “Coupling of Substructures for Dynamic Analysis,” *AIAA Journal,* vol. 6, pp. 1313-1319, 1968.

[5] T. Roland, Modeling and Identification of Linear Parameter-Varying Systems, Springer Verlag Heidelberg, 2010.

[6] N. Higham, The Singular Value Decomposition, The Princeton Companion to Applied Mathematics, Princeton University Press, 2015.

[7] E. Cardoso-Bihlo and A. Bihlo, “Exactly conservative physics-informed neural networks and deep operator networks for dynamical systems,” *Neural Networks,* vol. 181, 2025.

[8] A. Baez and W. Zhang, “Guaranteeing Conservation Laws with Projection in Physics-Informed Neural Networks,” 2024.

[9] T. Deighan, “Multi-Physics Systems Simulation for Fusion,” [Online]. Available: https://www.nafems.org/publications/resource_center/bm_apr_24_6/.

[10] Y. Li, J. Yang, W. Liu, L. Wang and C. Liao, “Linear parameter-varying modeling and identification of lithium-ion battery for control-oriented applications,” *Journal of Power Sources,* vol. 507, 2021.

[11] P.-b. Qian and L.-f. Qian, “Improved Craig-Bampton method for transient analysis of structures with large-scale plastic deformation,” *Journal of Vibroengineering,* 2017.

[12] S. Cheon, S. Lee and J. Lee, “A system-level interface sampling and reduction method for component mode synthesis with varying parameters,” *Applied Mathematics and Computation,* vol. 476, 2024.

[13] N. Guérin and F. Thouverez, “Thermomechanical Component Mode Synthesis for blade casing interaction prediction,” in *ASME Turbo Expo 2017: Turbomachinery Technical Conference and Exposition*, 2017.

[14] S. Zucca and M. Gola, “Component modes synthesis applied to a thermal transient analysis of a turbine disc,” in *3rd Worldwide Aerospace Conference & Technology Showcase*, 2002.

[15] P. Saves and R. Lafage, “SMT 2.0: A Surrogate Modeling Toolbox with a focus on hierarchical and mixed variables Gaussian processes,” *Advances in Engineering Software,* vol. 188, 2024.

[16] “Systems and methods for generating reduced order models,” *US provisional patent application No 16/253,635,* 2019.

[17] S. Siegelmann, “Computational capabilities of recurrent NARX neural networks,” *IEEE Transationcs on Systems,* vol. 27.2, pp. 208-215.